JOURNAL OF SOLID STATE CHEMISTRY **130,** 213–222 (1997)
ARTICLE NO. SC977296

Control on the Copper Valence and Properties by Oxygen Content Adjustment in the $LaCuO_{3-y}$ System ($0 \leq y \leq 0.5$)

M. Karppinen,*,† H. Yamauchi,*,[1] H. Suematsu,* K. Isawa,‡ M. Nagano,‡ R. Itti,§ and O. Fukunaga ||

*Materials and Structures Laboratory, Tokyo Institute of Technology, Nagatsuta, Midori-ku, Yokohama 226, Japan; †Laboratory of Inorganic and Analytical Chemistry, Helsinki University of Technology, FIN-02150 Espoo, Finland; ‡Research and Development Center, Tohoku Electric Power Co., Inc., Sendai 981, Japan; §Suranaree University of Technology, Nokhon Ratchasima 30000, Thailand; and || Department of Inorganic Materials, Tokyo Institute of Technology, Ookayama, Meguro-ku, Tokyo 152, Japan

Received September 10, 1996; in revised form January 27, 1997; accepted January 28, 1997

The $LaCuO_{3-y}$ perovskite is considered as the first member of the $01(n-1)n$ series of "layered cuprates." Highly oxidized, stoichiometric $LaCuO_3$ is stabilized under very high oxygen pressures, and was synthesized in a cubic-anvil-type high-pressure apparatus at 5 GPa and 1400°C using excess amounts of $KClO_4$ as an external oxidizing agent. Upon heating under ambient pressure the rhombohedral high-pressure phase loses oxygen yielding tetragonal, monoclinic, and orthorhombic forms of $LaCuO_{3-y}$ as intermediate products before the final decomposition into La_2CuO_4 and CuO or Cu_2O around 800°C. All three oxygen-deficient $LaCuO_{3-y}$ phases could be isolated and their stability limits and corresponding oxygen contents conveniently investigated by annealing stoichiometric $LaCuO_3$ in a thermobalance of high sensitivity in order to *in situ* detect the exact amount of oxygen loss. The nominal copper valence values calculated from the oxygen contents are compared and discussed with XPS data as well as with the results evaluated from magnetic susceptibility measurements.

1. INTRODUCTION

The structures of the existing high T_c superconducting cuprates can be designated as $M-m2(n-1)n$, where m tells the number of consecutively stacked M cation layers in the charge-reservoir block between the adjacent infinite-layer blocks. The second entry in this number series tells the number of spacing alkaline earth or rare oxide layers which are located between the charge-reservoir and infinite-layer blocks, while the fourth and third entries, respectively, correspond to the number of conducting CuO_2 planes and the number of bare alkaline earth or rare earth layers separating these CuO_2 planes in one infinite-layer block. So far, superconducting cuprate structures with $m = 0$, 1, 2, or 3 and n extending even up to 7 have been discovered with various cation constituents (M) in the charge-reservoir block (1). In finding new superconducting structures, the fact worthy of note is that the parent $01(n-1)n$ series of structures has not yet been "superconducterized."

The oxygen-defect $LaCuO_{3-y}$ perovskite (2) with alternating La–O and CuO_2 planes is thought to be the simplest member of the $01(n-1)n$ series, and is classified by the notation of 0101. The perovskite-type framework of $LaCuO_{3-y}$ is stable over a remarkably wide oxygen stoichiometry range, i.e., $0 \leq y \leq 0.5$, enabling the tuning of the nominal copper valence continuously from $+2$ to $+3$ (3,4). Furthermore, by doping the trivalent La site by divalent Sr, the Cu valence can be raised even above $+3$ (5,6). As shown in Table 1, several distinct structures in the $LaCuO_{3-y}$ system have been established depending on the synthesis pressure and the oxygen content of the product. Especially, the end stoichiometries of the perovskite structure show exceptional and interesting features in terms of possible superconductivity, i.e., three-dimensionality ($y = 0$) and a so-called two-leg ladder structure ($y = 0.5$) (7).

Formation of the highly oxidized, stoichiometric $LaCuO_3$ is promoted by very high oxygen pressures (8–10). The first $LaCuO_3$ samples were successfully synthesized by Demazeau *et al.* (2) from prereacted La_2CuO_4 and CuO powders at 6.5 GPa. Since then the high-pressure synthesis of $LaCuO_3$ has been accomplished as well when starting from the binary oxides (11,12) or from citrate gel precursors (5). The high oxygen pressures required have been generated *in situ* by the thermal decomposition of either $KClO_3$ (2,11), KO_2 (12), or CrO_3 (13). The high-pressure form of $LaCuO_3$ exhibits rhombohedrally distorted perovskite structure (2,12) in which the cations are at the centers of symmetry, but the oxygen has moved from its ideal position to ease the stress around the too-large Cu(+III) atoms. The tetragonal, low-pressure form of $LaCuO_{3-y}$ is stabilized for $0 < y < 0.2$, and has been synthesized by Bringley *et al.* (3,4) from coprecipitated, gelatinous lanthanum and copper hydroxide

[1] To whom correspondence should be addressed: Fax: 81-45-921-6953. E-mail: yamauchi@materia.titech.ac.jp.

0022-4596/97 $25.00

TABLE 1
Summary of the Synthesis and Structures of the (La, M)$_x$Cu$_y$O$_z$ Phases with $x = y$

Stoichiometry [synthesis]	Ref.	Space group	Cell volume (Å^3)	Cu–O bond lengths (Å)	BVS	Nominal Cu-valence
$LaCuO_3$ [La_2CuO_4, CuO, $KClO_3$, 6.5 GPa, 900°C]	2	*R*3*c*	57.75	1.94 × 6	+ 2.96	+ 3.00
$(La_{0.75}Sr_{0.25})CuO_3$ (amorphous prec., 7 GPa, 1000°C]	5	*R*3*c*	57.53			+ 3.25
$LaCuO_{2.95}$ [La- and Cu-hydroxide, 0.1 GPa O_2, 900°C]	3, 4	*P*4/*m*	57.93	1.909 × 4 1.986 × 1.9	+ 2.98	+ 2.90
$LaCuO_{2.67}$ [$LaCuO_{2.95}$, O_2, 525°C]	16	*P*2/*m*	57.19	Average 0.34 × Cu(1): 1.92 × 2 2.00 × 2 2.09 × 2 0.33 × Cu(2) 1.92 × 2 1.98 × 1 2.02 × 1 2.13 × 1 0.33 × Cu(2′) 1.92 × 2 1.99 × 1 2.00 × 1 2.14 × 1	+ 2.30 + 2.54 + 2.18 + 2.18	+ 2.34
$LaCuO_{2.50}$ [$LaCuO_{2.95}$, Ar, 450°C]	17	*Pbam*	56.39	1.920 × 1 1.941 × 2 1.962 × 1 2.260 × 1	+ 2.18	+ 2.00
$La_2Cu_2O_5$ [La_2O_3, CuO, air, 1000°C]	20	*C*2/*c*	58.12	Average 1 × Cu(1): 1.86 × 1 1.89 × 1 1.93 × 1 1.95 × 1 2.43 × 2 1 × Cu(2): 1.90 × 1 1.94 × 1 1.97 × 1 2.01 × 1 1 × Cu(3): 1.88 × 1 1.92 × 1 1.96 × 1 2.10 × 1	+ 2.08 + 2.43 + 1.91 + 1.89	+ 2.00
$LaCuO_{2.5}$ [$La_2Cu_2O_5$, 6 GPa, 900°C]	7	*Pbam*	56.34	1.941 × 2 1.966 × 2 2.285 × 1	+ 2.10	+ 2.00

TABLE 1—*Continued*

Stoichiometry [synthesis]	Ref.	Space group	Cell volume (Å^3)	Cu–O bond lengths (Å)	BVS	Nominal Cu-valence
$(La_{0.8}Sr_{0.2})_8Cu_8O_{19.84}$ [La_2O_3, $SrCO_3$, CuO, air, 1000°C]	23	*P*4/*mbm*	56.71	Average 1 × Cu(1): 1.932 × 2 2.038 × 3.68 1 × Cu(2): 1.906 × 2 1.932 × 2 2 × Cu(3): 1.860 × 2 1.932 × 2 2.395 × 1	+ 2.31 + 2.40 + 2.09 + 2.38	+ 2.16
$(La_{0.8}Sr_{0.2})CuO_{2.5}$ [$[La_{0.8}Sr_{0.2}]_8Cu_8O_{19.84}$, 6 GPa, 900°C]	7	*Pbam*	53.12	1.876 × 2 1.937 × 2 2.213 × 1	+ 2.41	+ 2.20
$(La_{0.86}Sr_{0.14})_4Cu_4O_{10}$ [La_2O_3, $SrCO_3$, CuO, O_2, 1025°C]	24	*Pbam*	56.09	1.930 × 1 1.969 × 1 1.936 × 2 2.213 × 1	+ 2.20	+ 2.14
$(La_{0.83}Sr_{0.17})_5Cu_5O_{13.04}$ [$[La_{0.83}Sr_{0.17})_8Cu_8O_{20}$, O_2-HIP 300 atm, 600°C]	25	*P*4/*m*	56.75	Average 1 × Cu(1): 1.911 × 2 2.003 × 4 4 × Cu(2): 1.832 × 1 2.034 × 1 1.912 × 2 2.256 × 1 2.256 × 1	+ 2.40 + 2.73 + 2.32	+ 2.39
$La_4BaCu_5O_{13.16}$ [La_2O_3, $BaCO_3$, CuO, air, 1000°C]	26	*P*4/*m*	57.72	Average 1 × Cu(1): 1.930 × 2 2.039 × 4 4 × Cu(2): 1.656 × 0.08 1.875 × 1 1.880 × 1 1.935 × 2 2.272 × 1	+ 2.47 + 2.53 + 2.46	+ 2.46
$La_4BaCu_5O_{12.5}$ [$La_4BaCu_5O_{13}$, N_2, 780°C]	27	mono	57.79			+ 2.20
$LaCuO_2$ [La_2O_3, Cu_2O, N_2, 1000°C]	28	*R*3*m*				+ 1.00
$LaCuO_{2.65}$ [$LaCuO_2$, O_2, 450°C]	29					+ 2.30

Note. The bond-valence-sums around Cu atoms have been calculated using a R_0 constant of 1.679 and the formulas of Brown and Altermatt (31).

precursors at oxygen pressures two orders of magnitude lower (0.04–0.1 GPa) than that required to prepare the rhombohedral form. The tetragonal distortion of the ideal perovskite structure is caused by a slight Jahn–Teller-like elongation of the CuO_6 octahedra. According to Webb *et al.* (14) the tetragonal phase can be obtained also by heating the rhombohedral form to 408°C under an ambient pressure. This observation has, however, aroused some controversy (4, 15).

The tetragonal $LaCuO_{3-y}$ phase starts to lose oxygen even near room temperature without an oxygen over-pressure. Below the oxygen deficiency of $y \sim 0.2$, the ordering of the oxygen vacancies in the (001) plane results in a new monoclinic supercell (16), and in the oxygen-deficient phase below $y \sim 0.4$ the oxygen-vacancy ordering, which is complete at $y = 0.5$, creates an orthorhombic cell (3, 4, 17). The oxygen sublattice in the orthorhombic $LaCuO_{2.5}$ phase is isomorphous with that of the $CaMnO_{2.5}$ structure (18, 19), which means that the corner-sharing CuO_5 pyramids are isolated in pairs into two-leg ladders running perpendicular to the (001) plane. The apical oxygen atoms, being directed outward of the ladders, are kept at a long distance from the Cu(+II) atoms due to a strong Jahn–Teller splitting, while the Cu–O bonds within the ladder are much shorter (7). The oxygen-deficient $LaCuO_{2.5}$ phase can also be synthesized directly by pressing normal-pressure $La_2Cu_2O_5$ material (20, 21) at 6 GPa (7). In order to dope the copper–oxygen ladders with holes, divalent-Sr-to-trivalent-La substitutions have been successfully applied [7]. In that case appropriate mixtures of $La_2Cu_2O_5$ and $(La_{0.8}Sr_{0.2})_8Cu_8O_{19.84}$ (22, 23) were used as starting materials for the high-pressure synthesis. Orthorhombic $CaMnO_{2.5}$ structure has been reported also for a normal-pressure synthesized sample with a stoichiometry of $(La_{0.86}Sr_{0.14})_4Cu_4O_{10}$ (24). Comparison between the calculated unit cell volumes (Table 1) shows, however, that the high-pressure synthesized $(La_{0.8}Sr_{0.2})CuO_{2.5}$ material is ca. 5% more dense than the ambient-pressure $(La_{0.86}Sr_{0.14})_4Cu_4O_{10}$ sample. On the other hand, O_2–HIP-treated (300 atm) $(La_{0.83}Sr_{0.17})_8Cu_8O_{20}$ material exhibits a new tetragonal $(La_{0.83}Sr_{0.17})_5Cu_5O_{13.04}$ structure (25) with homogeneously distributed lanthanum and strontium and a fixed oxygen content, in contrast to the $La_4BaCu_5O_{13-y}$ system in which the La and Ba atoms are ordered but the oxygen stoichiometry may vary, i.e. $0 \leq y \leq 0.5$ (26, 27). Finally, below the oxidation state of Cu(+II) the oxygen defect perovskite structure is not stable anymore, but the synthesis starting from La_2O_3 and Cu_2O results under a nitrogen atmosphere in the $LaCuO_2$ delafossite (28). The delafossite structure, consisting of triangular planes of O–Cu(+I)–O sticks, remains stable even upon oxidizing the copper to valences exceeding +II (29).

All the attempts to "superconducterize" the $LaCuO_{3-y}$ system, so far being mainly cation substitution studies on the fully oxidized ($y = 0$) (15, 30) or the fully oxygen-depleted ($y = 0.5$) (7) phases, have been unsuccessful. Since the defect-perovskite $LaCuO_{3-y}$ framework is stable over a remarkably wide oxygen stoichiometry range, carrier concentration should be able to be adjusted by a careful control of the oxygen content as well. In any case, systematic doping studies involving oxygen stoichiometry tuning in the $LaCuO_{3-y}$ system are supposed to provide interesting reference material for better understanding of the concept of "extended copper valency" and high T_c superconductivity. In the present contribution, fully oxidized $LaCuO_3$ material with the rhombohedral structure was first synthesized at 1400°C and 5 GPa using $KClO_4$ as an oxygen generator. Next, the oxygen stability and the thermal decomposition of the high-pressure form were investigated by means of thermogravimetry, and finally a series of oxygen-deficient $LaCuO_{3-y}$ samples was obtained by annealing $LaCuO_3$ material at different temperatures in flowing O_2 or Ar atmospheres. Performing the postannealings in a thermobalance allowed *in situ* determination of the magnitude of the resulting oxygen deficiency, y. For the characterization of the samples, XRD, SQUID, and XPS measurements were applied.

2. EXPERIMENTAL

The high-pressure synthesis of $LaCuO_3$ was carried out in a cubic-anvil-type apparatus using stoichiometric amounts of La_2O_3 and CuO as starting materials and 100% excess of $KClO_4$ as an external oxygen generator. Details of the synthesis optimization have been reported in (32, 33). The La_2O_3 powder was fired in air at 1000°C prior to use in order to remove absorbed moisture and CO_2. Lanthanum and copper oxides were first mixed thoroughly, since after the addition of the oxidizer only very gentle mixing could be applied due to the easy decomposition of $KClO_4$. The resulting mixture of the raw materials was tightly packed into a gold capsule. Pressure was applied through a pyrophyllite container with an internal graphite tube heater. The gold capsule, placed inside the heater, was electrically isolated from the graphite wall by means of a BN sleeve. The high pressure (4–5 GPa) was first slowly (in 30 min) applied, and then the temperature was increased to 1400°C in 10 min. The sample was treated in the high-pressure and high-temperature conditions for 30 min, and afterward quenched to room temperature in 10 s. Finally, the pressure was decreased to ambient value in 30 min.

The oxygen evolution characteristics and the thermal decomposition of the high-pressure $LaCuO_3$ phase under oxygen and argon atmospheres were studied up to 950°C using a thermogravimetric apparatus (MAC Science TG/DTA 2000S) equipped with an infrared furnace. The sample mass was around 20 mg and the heating rate was $2°C\,min^{-1}$. Several oxygen-deficient $LaCuO_{3-y}$ samples were prepared in the same thermobalance by heating

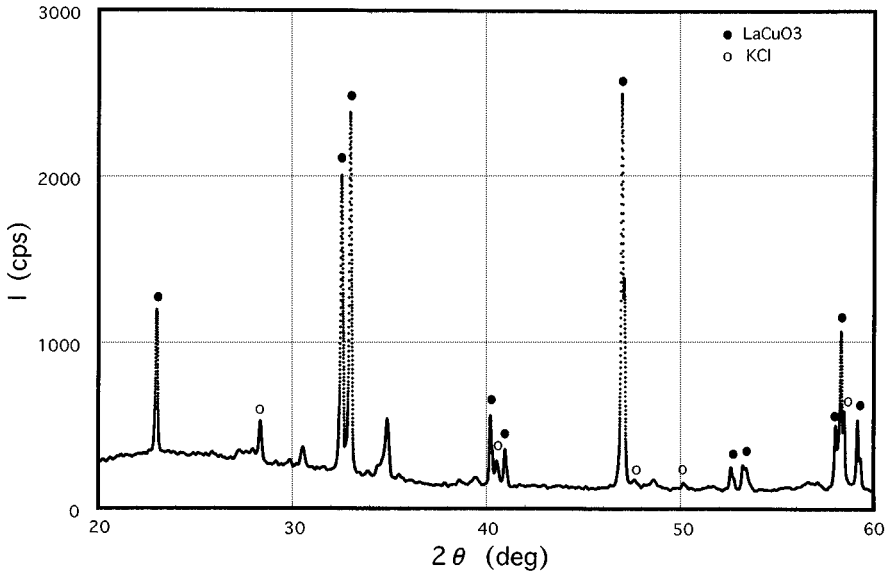

FIG. 1. X-ray diffraction pattern for the high-pressure (5 GPa, 1400°C) synthesis product (33). The reflection peaks due to rhombohedral $LaCuO_3$ (●) and KCl (○) are indicated.

($2^\circ C\ min^{-1}$) as-synthesized $LaCuO_3$ material (ca. 5–15 mg) in a flowing argon or oxygen atmosphere to temperatures between 200 and 820°C with an isothermal period of 30–180 min at the final temperature in order to make certain of the equilibrium conditions.

The phase content of the synthesized $LaCuO_{3-y}$ samples was checked by an X-ray diffractometer (MAC Science M18XHF) using Cu$K\alpha$ radiation. Magnetic measurements were carried out with a SQUID magnetometer (Quantum Design MPMSR 5S) down to 5 K. For the photoelectron spectroscopic (XPS) measurements an ultrahigh-vacuum system (typical pressure 2×10^{-10} Torr) equipped with an Al X-ray source (1486.6 eV) was used. Sample powder was pasted onto the sample holder using conductive carbon tape. All the measurements were carried out at room-temperature. The energy distribution of the photoelectrons was determined with a resolution of 0.7 eV, and the C 1*s* peak at 285.0 eV was used as a reference for the obtained core-level binding energies.

3. RESULTS AND DISCUSSION

The high-pressure synthesis at 1400°C and 5 GPa oxygen pressure yielded the $LaCuO_3$ perovskite material with the rhombohedral structure as a main phase. Judging from the X-ray diffraction data, the high-pressure synthesis product was free from the starting oxides and traces of the La_2CuO_4 phase. No indication of the very stable $La(OH)_3$ compound, often found as an impurity phase (12, 15), could be seen in the XRD patterns. On the other hand, unidentified impurity peaks at $2\theta = 30.5$ and 34.9° as well as peaks due to KCl, formed as a by-product due to the decomposition of $KClO_4$, were always present (Fig. 1). Synthesis product after the 4 GPa treatment at 1400°C was found to be a mixture of the rhombohedral and tetragonal $LaCuO_{3-y}$ phases.

A. Thermal Stability and Oxygen Stoichiometry

The oxygen evolution characteristics and the thermal decomposition of the rhombohedral $LaCuO_3$ were studied in oxygen and argon atmospheres (Fig. 2). Upon heating the

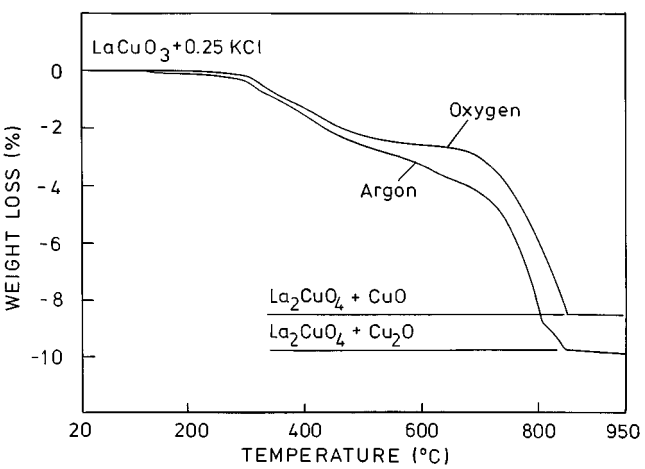

FIG. 2. Oxygen evolution and thermal decomposition of the high-pressure synthesized $LaCuO_3$ material in O_2 and Ar (33).

oxygen evolution starts above 200°C in both atmospheres. The reflection points seen in the TG curves at ca. 300 and 450°C (in Ar) were attributed to the structural phase transitions, discussed in the Introduction. Above 700°C the final decomposition of the $LaCuO_{3-y}$ framework and the evaporation of KCl, present in the high-pressure product used as a starting material in TG experiments, overlap. Judging from the magnitude of the total weight loss and the XRD data of the TG residues, KCl is totally removed from the studied samples during the TG runs up to 950°C. In oxygen, the decomposition of $LaCuO_{3-y}$ into the La_2CuO_4 and CuO phases occurs above 820°C, while in argon the decomposition is already completed and the Cu(II) oxide further reduced to Cu_2O around 800°C.

Various oxygen-deficient $LaCuO_{3-y}$ samples were prepared by annealing high-pressure synthesized $LaCuO_3$ material in argon and oxygen atmospheres to temperatures between 200 and 820°C. The postannealings were performed in a thermobalance of high sensitivity in order to follow the oxygen depletion process and to determine the exact amount of oxygen loss. Examples of these TG curves are shown in Fig. 3. The oxygen deficiences in the $LaCuO_{3-y}$ annealing products were calculated from the TG data by supposing that the starting material contains the $LaCuO_3$ and KCl phases in the nominal ratio. Parallel experiments yielded the y values with the reproducibility of ± 0.01, but the accuracy of the method was estimated at ± 0.04 due to the possible systematic shift caused by the presence of impurity phases (other than KCl) in the starting material. The reflections in the XRD patterns of the resulting $LaCuO_{3-y}$ samples were compared with the data reported by Bringley *et al.* (3,4) for the tetragonal, monoclinic, and orthorhombic phases. The observed phase contents together with the corresponding oxygen-deficiency and Cu-valence values are summarized in Table 2. The XRD patterns of the samples annealed in Ar at 400 and 500°C could be readily indexed according to the monoclinic and orthorhombic structures, respectively. The oxygen-deficiency values in the same order are $y = 0.39$ and 0.50.

The tetragonal structure, although appearing as an intermediate phase in the samples annealed at 240–320°C, was found to be difficult to isolate in a single-phase form. Especially, stoichiometric $LaCuO_3$ material with the tetragonal structure cannot be obtained by the present normal-pressure annealing route from the rhombohedral $LaCuO_3$ phase, since the rhombohedral-to-tetragonal phase transition does not occur at temperatures lower than the onset temperature of oxygen depletion. Whether tetragonal $LaCuO_{3-y}$ with $y = 0$ exists in general, is still an open question (4). According to the continuous TG runs, the stability region of the tetragonal structure in an Ar atmosphere seems to extend up to 310–320°C if judged from the position of the first reflection point. However, careful mapping of the tetragonal-to-monoclinic phase transition region at 240–340°C by means of TG runs with a long (30–180 min) isothermal heating period at the final temperature (Fig. 3b, Table 2) reveals that the tetragonal phase is stable at most only up to 260°C. After the long annealings (180 min) the oxygen content saturates at 240–260°C to the level of the reflection point in the continuous TG runs, i.e., around $y = 0.2$. The phase-transition temperatures observed in the present study are in general agreement with those reported by Bringley *et al.* (4) for the tetragonal-to-monoclinic (ca. 400°C) and for the monoclinic-to-orthorhombic (ca. 600°C) transitions.

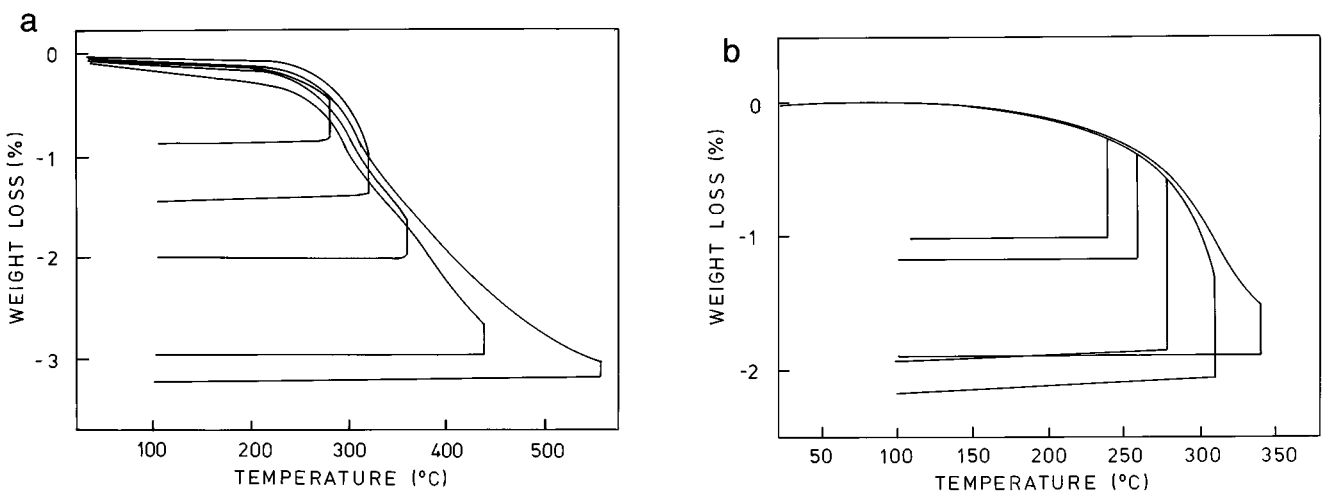

FIG. 3. Examples of TG curves for the controlled oxygen depletion of the high-pressure synthesized $LaCuO_3$ material in Ar, with an isothermal period of 30 (a) or 180 (b) min at the final annealing temperature.

TABLE 2

TG and XRD Data on the Oxygen Deficiency *y*, Corresponding Nominal Cu-Valence, and the Phase Content of the $LaCuO_{3-y}$ Samples Annealed in Ar and O_2 (Indicated by *) Atmospheres at Various Temperatures for 30–180 min

T(°C)	Time (min)	y	Cu-valence	Phase
200	30	0.00	+ 3.00	rhombo
210*	180	0.00	+ 3.00	rhombo
240	180	0.15	+ 2.70	tetra (+rhombo)
260	180	0.18	+ 2.64	tetra (+rhombo)
280	30	0.13	+ 2.74	tetra (+rhombo)
280	180	0.28	+ 2.44	tetra (+rhombo, mono)
280*	30	0.12	+ 2.76	tetra (+rhombo)
300	180	0.28	+ 2.44	tetra (+rhombo, mono)
300	30	0.17	+ 2.66	tetra (+rhombo)
310	180	0.33	+ 2.34	tetra (+mono)
320	30	0.23	+ 2.54	tetra (+rhombo)
340	30	0.29	+ 2.42	mono (+tetra)
360	30	0.31	+ 2.38	No XRD data
400	30	0.39	+ 2.22	mono
400*	30	No TG data		mono
440	30	0.47	+ 2.06	mono (+ortho)
500	30	0.50	+ 2.00	ortho
500*	30	0.41	+ 2.18	mono
560	30	0.51	+ 1.98	ortho
560*	30	No TG data		mono
640	30	No TG data		ortho
640*	30	No TG data		mono (+ortho)
700*	30	No TG data		ortho (+mono)
740*	30	No TG data		ortho
820*	30	No TG data		ortho

B. XPS Study

XPS measurements were performed on three $LaCuO_{3-y}$ samples with oxygen deficiencies y of 0 (rhombo), 0.39 (mono), and 0.50 (ortho). In each sample studied the Cu $2p_{3/2}$ main peak was found at 933.2 eV (Fig. 4). In literature, the following binding energies (BE) have been reported for Cu(+III) compounds: 933.5–936.7 eV in $LaCuO_3$ (5, 13); 932.7–934.6 eV in $NaCuO_2$ (34, 35); 934.7 eV in $La_2Li_{0.5}Cu_{0.5}O_4$ (36); and 934.2–934.9 eV in $YBa_2Cu_3O_{7-d}$ (37–39). For comparison, in CuO the corresponding value varies in the range 933.1–934.1 eV (5, 40, 41). The discrepancies in the observed values, especially among different studies, can be partly explained by calibration problems. Also, the oxygen coordination of copper and the localization/delocalization character of the Cu–O bond electrons play important roles in determining the BE values. In $NaCuO_2$ and $YBa_2Cu_3O_{7-d}$ trivalent copper exhibits a square–planar coordination, while in $La_2Li_{0.5}Cu_{0.5}O_4$ (tetrahedrally distorted) as well as in the stoichiometric $LaCuO_3$ the oxygen environment of copper is octahedral. In the $(La_{1-x}Sr_x)CuO_3$ system, formal Cu valence values higher than + III are achieved. Darracq *et al.* (13) have carried out an XPS study on a sample with $x = 0.2$ and fitted the resulting spectrum with two Cu $2p_{3/2}$ main peaks. The BE value close to 933.1 eV was assigned to Cu(+III), and the peak in the higher energy side (935.3 eV) was supposed to arise from Cu(+IV).

The photoelectron intensity of the Cu $2p_{3/2}$ satellite peak at 943.0 eV was found to decrease with increasing oxygen deficiency y in $LaCuO_{3-y}$. The intensity of the satellite peak relative to the intensity of the main peak was 69, 46, and 35% for the samples with $y = 0$, 0.39, and 0.50, respectively. This observation might reflect the actual decrease of copper valence with proceeding reduction. In the case of superconducting cuprates the intensity of the satellite peak is usually 40–45% of that of the main peak in *p*-type (Cu-valence $\sim +2.15$) and around 30% in *n*-type (Cu-valence $\sim +1.85$) phases (42). Also, according to configuration–interaction (CI) calculations performed by Mizokawa *et al.* (35) for square–planar $(Cu^{3+}O_4^{2-})^{5-}$ clusters (D_{4h} symmetry) the contribution of d^8 configuration [Cu(+III)] is stronger for the satellite peak than for the main peak, while the opposite applies in the cases of d^9L[Cu(+II)] and $d^{10}L^2$[Cu(+I)] configurations.

The O 1*s* spectrum of stoichiometric $LaCuO_3$ consists of a peak at 531.3 eV with a weak shoulder in the lower energy side (Fig. 5). In the oxygen-deficient samples of $y = 0.39$ and 0.50, the main peak shifts to slightly higher binding energies, i.e., to 531.6 and 531.8 eV, respectively. With decreasing oxygen content the intensity of the shoulder at 529.1 eV rapidly increases. It is noted that in high T_c cuprates only single O 1*s* peak is observed around 528–529 eV (43). The fact that the 529 eV O 1*s* peak becomes prominent with decreasing Cu valence value in $LaCuO_{3-y}$ suggests that the chemical environment of oxygen resembles that of superconducting cuprates when the nominal Cu valence is closer to +II than to +III.

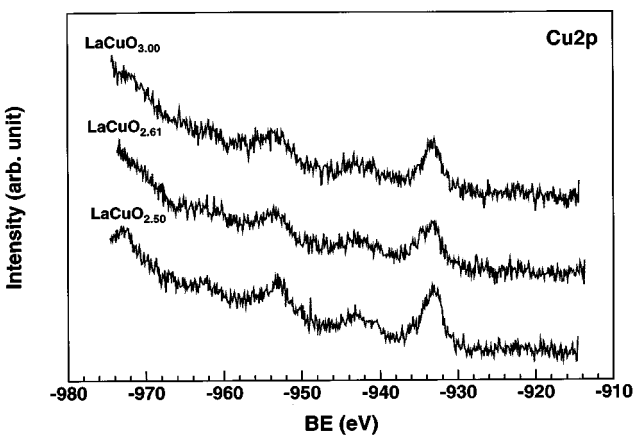

FIG. 4. Cu 2*p* XPS spectra for $LaCuO_{3-y}$ samples with $y = 0$, 0.39, and 0.50.

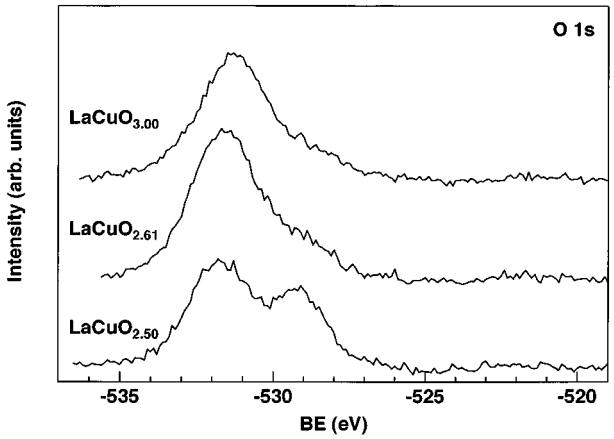

FIG. 5. O 1*s* XPS spectra for $LaCuO_{3-y}$ samples with $y = 0$, 0.39, and 0.50.

In the case of lanthanum the presence of two different environments is evident. The obtained La 3*d* spectra (Fig. 6) can be interpreted by assuming two overlapping doublets both in the $3d_{5/2}$ (832–840 eV) and in the $3d_{3/2}$ (848–857 eV) area. The rhombohedral distortion in the stoichiometric $LaCuO_{3-y}$ ($y = 0$) splits the 12 La–O bonds into 3 short (2.495 Å), 6 intermediate (2.733 Å), and 3 long (3.012 Å) bonds (12). The La 3*d* spectrum of the rhombohedral $LaCuO_{3.00}$ sample consists mainly of single component corresponding to the environment described above. While increasing the oxygen deficiency y from 0 to 0.5 in $LaCuO_{3-y}$ the coordination number of lanthanum changes from 12 to 10. As the reduction proceeds, the intensity of the other $3d_{5/2}$ and $3d_{3/2}$ doublets increases. In the $LaCuO_{2.50}$ sample this contribution, originating from the 10-fold-coordinated La(+III) ions, is dominant.

C. Magnetic Properties

Examples of magnetic susceptibility versus temperature curves measured in a SQUID magnetometer for the $LaCuO_{3-y}$ samples ($y = 0$, 0.13, 0.23, 0.29, and 0.51) are shown in Fig. 7. For each sample, a weak ferromagnetic behavior was observed below 20 K. Bringley *et al.* (4) have reported a same kind of behavior at slightly higher temperatures for the tetragonal $LaCuO_{3-y}$ phase. The fact that the T_N of the magnetic transition was found to be essentially independent of the oxygen deficiency y suggests that, in our case at least, some impurity phase might contribute to the result. Above 20 K the susceptibility data could be fitted to a Curie–Weiss type behavior with the expression of $X = X_0 + C/(T - \theta)$. In each case the obtained absolute value for the Weiss constant (θ) was very small. The fitted Curie constants (C) and temperature-independent susceptibilities (X_0) as well as the calculated effective magnetic moments (μ_{eff}) are summarized in Table 3. Trivalent lanthanum ($4f^0$) has no spin, and if trivalent copper ($3d^8$) is supposed to be in a low-spin state the increase seen in the magnetic susceptibility curves at low temperatures is due to divalent copper ($3d^9$) with one unpaired electron per atom ($\mu_{theor} = 1.73$ μB). The observed μ_{eff} value of 0.43 μB in the $LaCuO_{2.49}$ sample thus corresponds to approximately 6% free Cu^{2+} spins. Since μ_{eff} does not show any real trend in respect to the (nominal) average Cu-valence value, it is probable that the impurity phase contributes strongly to the result. On the other hand, the fluoride system M_3CuF_6 (M = alkaline metal) is an example of high-spin Cu(+III) ($\mu_{theor} = 2.83$ μB) in octahedral coordination (44).

According to the electrical resistivity measurements of Bringley *et al.* (4) the orthorhombic $LaCuO_{2.5}$ phase is insulating. On the other hand, the original data of Demazeau *et al.* (2, 45) reveal the rhombohedral $LaCuO_3$ phase to

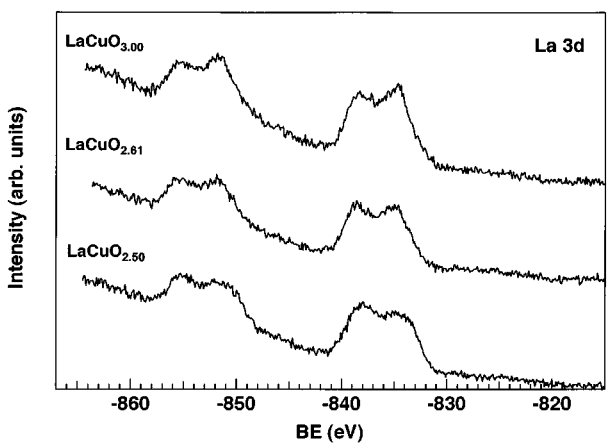

FIG. 6. La 3*d* XPS spectra for $LaCuO_{3-y}$ samples with $y = 0$, 0.39, and 0.50.

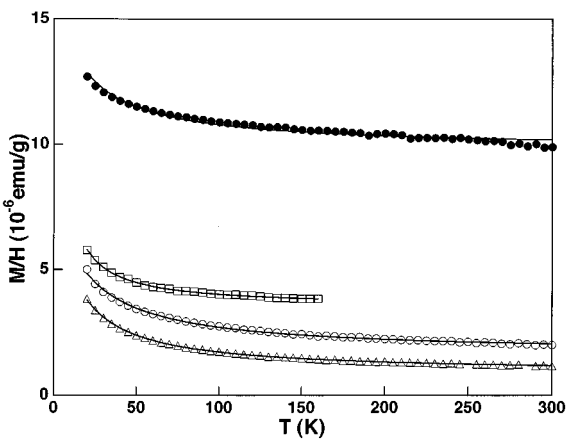

FIG. 7. Magnetic susceptibility data for $LaCuO_{3-y}$ samples with $y = 0$ (rhombo, ●), 0 (rhombo + tetra, □), 0.13 (tetra, ○), and 0.51 (ortho, △).

TABLE 3
Parameters Obtained by Fitting the Magnetic Susceptibility Data of Various $LaCuO_{3-y}$ Samples to the Curie–Weiss-like Behavior: Curie Constant C, Temperature-Independent Susceptibility X_0, and Effective Magnetic Moment μ_{eff}

y	Cu-valence	Phase content	X_0 $[10^{-6}\,emug^{-1}]$	C $[10^{-4}\,emuKg^{-1}]$	μ_{eff}/μ_B
0.00	+ 3.00	rhombo	3.52	0.50	0.31
0.00	+ 3.00	rhombo (+tetra)	1.66	1.24	0.50
0.13	+ 2.74	tetra (+rhombo)	9.84	1.09	0.47
0.23	+ 2.54	tetra (+rhombo)	1.00	1.30	0.51
0.29	+ 2.42	mono (+tetra)	1.87	1.77	0.59
0.51	+ 1.98	ortho	0.88	0.95	0.43

exhibit Pauli paramagnetism and metallic properties down to 77 K. Controversially, rhombohedral $LaCuO_3$ has also been reported to be an insulator (30, 46). The X_0 values obtained as present Curie–Weiss fitting results (Table 3) support the observations of Bringley *et al.* (4) and Demazeau *et al.* (2, 45). Supposing the temperature-independent contributions of the core diamagnetism and the Van Vleck paramagnetism to be constant through the whole oxygen stoichiometry range studied ($0.00 \le y \le 0.51$), the trend in X_0 indicates that the Pauli-like magnetic susceptibility and thus the carrier concentration is smallest in the $y = 0.51$ sample (= insulating), and increases with increasing mixed Cu(+III)/(+II) valence, having a maximum in the oxygen-deficient tetragonal phase ($y = 0.13$).

4. CONCLUSIONS

High-pressure synthesis at 5 GPa and 1400°C yields nearly single-phase rhombohedral $LaCuO_3$ material. At 4 GPa the product was found to be a mixture of the rhombohedral and tetragonal phases. Oxygen-deficient $LaCuO_{3-y}$ samples with gradually changing (nominal) Cu-valence values were prepared by annealing the high-pressure synthesized material under normal pressure at various temperatures between 240 and 820°C. The mass of the samples synthesized in the existing high-pressure apparatus is characteristically too small to allow efficient oxygen content determination by means of conventional chemical analysis after the synthesis/postannealings. However, careful and convenient *in situ* control on the oxygen content of the synthesized oxygen-deficient $LaCuO_{3-y}$ samples was achieved by performing the postannealings in a thermobalance. The known tetragonal, monoclinic, and orthorhombic structures of $LaCuO_{3-y}$ were found as intermediates upon the removal of oxygen from the stoichiometric, rhombohedral $LaCuO_3$ phase. Although the monoclinic and orthorhombic forms were easily isolated by annealing in Ar at 400 and 500°C, respectively, the tetragonal structure was found to be more difficult to stabilize in a single-phase form. Finally, around 750–900°C, depending on the atmosphere, the pervoskite framework is decomposed into La_2CuO_4 and CuO/Cu_2O.

XPS measurements gave interesting results concerning the chemical state of copper, lanthanum, and oxygen in the $LaCuO_{3-y}$ system. The binding energies of the Cu $2p_{3/2}$ peaks were found to be insensitive to the changes in the mixed Cu(+III)/Cu(+II) valence, but the relative intensities of the main peak and the satellite peak might reflect the Cu valence state more visibly. In future, it would be interesting to test if the proposed trend can be seen in the cases of other high-valent cuprate systems as well, e.g., $NaCuO_2$, Sr_2CuO_{4-y}, and $(La, Sr)CuO_3$. The O 1*s* peak corresponding to the highest Cu valence is located at quite a large BE of 531.3 eV. With decreasing Cu valence this peak shifted slightly to even higher values, and simultaneously another peak around 529.1 eV arose. In the La 3*d* spectra the gradual change in the coordination polyhedron was seen as an overlap of two doublets corresponding to the extreme cases of 12- and 10-coordinated lanthanum.

Based on its chemical and structural properties, in many aspects highly related to those of the cuprate superconductors, the oxygen-defect $LaCuO_{3-y}$ perovskite framework has been considered as a potential candidate for exhibiting superconductivity when optimally doped. Judging from the behavior of the temperature-independent susceptibility, the orthorhombic $LaCuO_{2.5}$ phase is considered to be insulating, while the phases with the mixed Cu(+III)/(+II) valence, as well as the stoichiometric $LaCuO_3$, show larger carrier concentrations. Next, important points for consideration are (i) the three-dimensional character of the fully oxidized $LaCuO_3$ structure, (ii) the homogeneity/inhomogeneity of hole doping in the Cu–O sublattice consisting of alternating 5-fold and 6-fold coordinated copper atoms, and finally (iii) the fact that if we suppose nearly perfect CuO_2 planes in the $LaCuO_{3-y}$ system, it will be much more oxidized in terms of (nominal) Cu-valence than the cuprates so far showing superconductivity, or vice versa. By a combination of oxygen content adjustment and partial

tetravalent substitution on the trivalent La-site it might, however, be possible to optimize the $LaCuO_{3-y}$ system in respect to possible superconductivity.

ACKNOWLEDGMENTS

Professor Itoh of Tokyo Institute of Technology is thanked for providing technical help. Financial support by a Grant-in-Aid for Scientific Research under Contract 08455299 from The Ministry of Education, Science and Culture of Japan as well as by the Mitsubishi Foundation is gratefully acknowledged.

REFERENCES

1. H. Yamauchi and M. Karppinen, "Superlattices and Microstructures," in press.
2. G. Demazeau, C. Parent, M. Pouchard, and P. Hagenmuller, *Mater. Res. Bull.* **7,** 913 (1972).
3. J. F. Bringley, B. A. Scott, S. J. LaPlaca, R. F. Boehme, T. M. Shaw, M. W. McElfresh, S. S. Trail, and D. E. Cox, *Nature* **347,** 263 (1990).
4. J. F. Bringley, B. A. Scott, S. J. LaPlaca, T. R. McGuire, F. Mehran, M. W. McElfresh, and D. E. Cox, *Phys. Rev. B* **47,** 15,269 (1993).
5. S. Darracq, S. G. Kang, J. H. Choy, and G. Demazeau, *J. Solid State Chem.* **114,** 88 (1995).
6. S. Darracq, G. Demazeau, and A. Largeteau, *Solid State Commun.* **94,** 629 (1995).
7. Z. Hiroi and M. Takano, *Nature* **377,** 41 (1995).
8. O. M. Sreedharan, C. Mallika, and K. Swaminathan, *J. Mater. Sci.* **23,** 2735 (1988).
9. A. Dwivedi, M. A. Rodriguez, and A. N. Cormack, *J. Am. Ceram. Soc.* **75,** 1993 (1992).
10. M. R. Chandrachood, K. K. Singh, D. E. Morris, and A. P. B. Sinha, *Physica C* **241,** 319 (1995).
11. A. W. Webb, E. F. Skelton, S. B. Qadri, E. R. Carpenter, Jr., M. S. Osofsky, R. J. Soulen, and V. LeTourneau, *Physica C* **162,** 899 (1989).
12. C. Weigl and K. J. Range, *J. Alloys Cmpd.* **200,** L1 (1993).
13. K. Allan, A. Campion, J. Zhou, and J. B. Goodenough, *Phys. Rev. B* **41,** 11,572 (1990).
14. A. W. Webb, E. F. Skelton, S. B. Qadri, E. R. Carpenter, Jr., M. S. Osofsky, R. J. Soulen, and V. LeTourneau, *Phys. Lett. A* **137,** 205 (1989).
15. A. W. Webb, E. F. Skelton, S. B. Qadri, and E. R. Carpenter, Jr., *J. Solid State Chem.* **102,** 519 (1993).
16. S. J. La Placa, J. F. Bringley, B. A. Scott, and D. E. Cox, *J. Solid State Chem.* **118,** 170 (1995).
17. S. J. La Placa, J. F. Bringley, B. A. Scott, and D. E. Cox, *Acta Crystallogr. C* **49,** 1415 (1993).
18. K. R. Poeppelmeier, M. E. Leonowicz, and J. M. Longo, *J. Solid State Chem.* **44,** 89 (1982).
19. K. R. Poeppelmeier, M. E. Leonowicz, J. C. Scanlon, J. M. Longo, and W. B. Yelon, *J. Solid State Chem.* **45,** 71 (1982).
20. R. J. Cava, T. Siegrist, B. Hessen, J. J. Krajewski, W. F. Peck, Jr., B. Batlogg, H. Takagi, J. V. Waszczak, and L. F. Schneemeyer, *Physica C* **177,** 115 (1991).
21. J. Geny, J. K. Meen, and D. Elthon, *in* "Proc. 10th Anniversary HTS Workshop on Physics, Materials and Applications, Houston, Texas, March 12–16, 1996," submitted.
22. Y. Tokura, J. B. Torrance, A. I. Nazzal, T. C. Huang, and C. Ortiz, *J. Am. Chem. Soc.* **109,** 7555 (1987).
23. L. Er-Rakho, C. Michel, and B. Raveau, *J. Solid State Chem.* **73,** 514 (1988).
24. K. Otzschi and Y. Ueda, *J. Solid State Chem.* **107,** 149 (1993).
25. K. Otzschi, A. Hayashi, Y. Fujiwara, and Y. Ueda, *J. Solid State Chem.* **105,** 573 (1993).
26. C. Michel, L. Er-Rakho, M. Hervieu, J. Pannetier, and B. Raveau, *J. Solid State Chem.* **68,** 143 (1987).
27. M. Kato, N. Kojima, K. Yoshimura, Y. Ueda, N. Nakayama, K. Kosuge, Z. Hiroi, and Y. Bando, *J. Solid State Chem.* **103,** 253 (1993).
28. H. Haas and E. Kordes, *Z. Kristallogr.* **129,** 259 (1969).
29. R. J. Cava, H. W. Zandbergen, A. P. Ramirez, H. Takagi, C. T. Chen, J. J. Krajevski, W. F. Peck, Jr., J. V. Waszczak, G. Meigs, R. S. Roth, and L. F. Schneemeyer, *J. Solid State Chem.* **104,** 437 (1993).
30. A. W. Webb, E. F. Skelton, S. B. Qadri, V. Browning, and E. R. Carpenter, Jr., *Phys. Rev. B* **45,** 2480 (1992).
31. I. D. Brown and D. Altermatt, *Acta Cryst. B* **41,** 244 (1985).
32. M. Karppinen, H. Yamauchi, T. Ito, H. Suematsu, and O. Fukunaga, *Mater. Sci. Eng. B* **41,** 59 (1996).
33. M. Karppinen, H. Yamauchi, H. Suematsu, and O. Fukunaga, *Physica C* **264,** 268 (1996).
34. P. Steiner, V. Kinsinger, I. Sander, B. Siegwart, S. Hufner, C. Politis, R. Hoppe, and H. P. Muller, *Z. Phys. B* **67,** 497 (1987).
35. T. Mizokawa, A. Fujimori, H. Namatame, K. Akeyama, and N. Kosugi, *Phys. Rev. B* **49,** 7193 (1994).
36. J. H. Choy, D. Y. Jung, S. J. Kim, Q. W. Choi, and G. Demazeau, *Physica C* **185/189,** 567 (1991).
37. H. Ihara, M. Hirabayashi, N. Terada, Y. Kimura K. Senzaki, M. Akimoto, K. Bushida, F. Kawashima, and R. Uzuka, *Jpn. J. Appl. Phys.* **26,** L460 (1987).
38. J. H. Choy, S. H. Byeon, S. T. Hong, D. Y. Jung, S. Y. Choy, B. W. Kim, J. T. Kim, D. Y. Noh, H. I. Yoo, D. N. Lee, D. Shung, and T. S. Park, *J. Korean Ceram. Soc.* **25,** 154 (1988).
39. A. F. Carley, M. Wyn Roberts, J. S. Lees, and R. J. D. Tilley, *J. Chem. Soc. Faraday Trans.* **86,** 3129 (1990).
40. G. Schon, *Surf. Sci.* **35,** 96 (1973).
41. J. Ghijsen, L. H. Tjeng, J. van Elp, H. Eskes, J. Westerink, G. A. Sawatzky, and M. T. Czyzyk, *Phys. Rev. B* **38,** 11,322 (1988).
42. R. P. Vasquez, *J. Electron Spectrosc. Relat. Phenom.* **66,** 209 (1994).
43. R. Itti, K. Isawa, J. Sugiyama, K. Ikeda, H. Yamauchi, N. Koshizuka, and S. Tanaka, *J. Phys. Chem. Solids* **54,** 1199 (1993).
44. R. Hoppe and G. Wingefeld, *Z. Anorg. Allg. Chem.* **519,** 195 (1984).
45. J. B. Goodenough, N. F. Mott, M. Pouchard, G. Demazeau, and P. Hagenmuller, *Mater. Res. Bull.* **8,** 647 (1973).
46. Y. Khan, *J. Mater. Sci. Lett.* **6,** 1387 (1987).